Published in final edited form as:
Circulation. 2014 September 9; 130(11): 880–891. doi:10.1161/CIRCULATIONAHA.114.010757.

CCR5 as a Treatment Target in Pulmonary Arterial Hypertension

Valérie Amsellem, PhD[1], **Larissa Lipskaia, PhD**[#1], **Shariq Abid, MD, PhD**[#1], **Lucie Poupel, PhD**[#2], **Amal Houssaini, PhD**[1], **Rozenn Quarck, PhD**[3], **Elisabeth Marcos, MSC**[1], **Nathalie Mouraret, PhD**[1], **Aurélien Parpaleix, MSC**[1], **Régis Bobe, PhD**[4], **Guillaume Gary-Bobo, PhD**[1], **Mirna Saker, MD**[1], **Jean-Luc Dubois-Randé, MD, PhD**[5], **Mark T Gladwin, MD, PhD**[6], **Karen A. Norris, PhD**[7], **Marion Delcroix, MD**[3], **Christophe Combadière, PhD**[2,8,9], and **Serge Adnot, MD, PhD**[1]

[1]Inserm U955 and Département de Physiologie, Hôpital Henri Mondor, Créteil, France, Université Paris-Est Créteil (UPEC), France

[2]Sorbonne Universités, UPMC Univ Paris 06, CR7, Centre d'Immunologie et des Maladies Infectieuses (CIMI-Paris), Paris, France

[3]Respiratory Division, University Hospitals of Leuven and Department of Clinical and Experimental Medicine, University of Leuven, Belgium

[4]Université Paris-Sud, Unité mixte de Recherche en Santé 770, Le Kremlin-Bicêtre, France

[5]Service de Cardiologie, Hôpital Henri Mondor, AP-HP, 94010, Créteil, France; Université Paris-Est Créteil (UPEC)

[6]Division of Pulmonary, Allergy and Critical Care Medicine, UPMC, Pittsburgh, PA

[7]Heart, Lung, Blood and Vascular, University of Pittsburgh, Pittsburgh, PA

[8]Inserm, U1135, CIMI-Paris, 91 Bd de l'hôpital, F-75013, Paris, France

[9]CNRS, ERL 8255, CIMI-Paris, 91 Bd de l'hôpital, F-75013, Paris, France

[#] These authors contributed equally to this work.

Abstract

Background—Pulmonary arterial hypertension (PH), whether idiopathic or related to underlying diseases such as HIV infection, results from complex vessel remodeling involving both pulmonary-artery smooth muscle cell (PA-SMC) proliferation and inflammation. CCR5, a co-receptor for cellular HIV-1 entry expressed on macrophages and vascular cells, may be involved in the pathogenesis of PH. Maraviroc is a new CCR5 antagonist designed to block HIV entry.

Methods and Results—Marked CCR5 expression was found in lungs from patients with idiopathic PH, in mice with hypoxia-induced PH and in SIV-infected macaques, in which it was chiefly localized in the PA-SMCs. To assess the role for CCR5 in experimental PH, we used both gene disruption and pharmacological CCR5 inactivation in mice. Because maraviroc does not bind

Correspondence: Serge Adnot, MD, PhD Hôpital Henri Mondor, Service de Physiologie-Explorations Fonctionnelles 94010, Créteil, France Phone: +33 149 812 677 Fax: +33 149 812 667 serge.adnot@inserm.fr.

Conflict of Interest Disclosures: None.

to murine CCR5, we used human-CCR5ki mice for pharmacological and immunohistochemical studies. Compared to wild-type mice, $CCR5^{-/-}$ mice or human-CCR5ki mice treated with maraviroc exhibited decreased PA-SMC proliferation and recruitment of perivascular and alveolar macrophages during hypoxia exposure. $CCR5^{-/-}$ mice reconstituted with wild-type bone-marrow cells and wild-type mice reconstituted with $CCR5^{-/-}$ bone-marrow cells were protected against PH, suggesting CCR5-mediated effects on PASMCs and macrophage involvement. The CCR5 ligands CCL5 and the HIV-1 gp120 protein increased intracellular calcium and induced growth of human and h-CCR5ki mouse PASMCs; maraviroc inhibited both effects. Maraviroc also reduced the growth-promoting effects of conditioned media from CCL5-activated macrophages derived from human-CCR5ki mice on PA-SMCs from wild-type mice.

Conclusions—The CCL5-CCR5 pathway represents a new therapeutic target in PH associated with HIV or with other conditions.

Keywords

hypertension pulmonary; inflammation; remodeling; CCR5; smooth muscle cells

Pulmonary arterial hypertension (PH) develops either as an idiopathic condition or in association with various underlying diseases such as collagen vascular disease, portal hypertension, or HIV infection [1-3]. The hallmark pathological feature of all forms of PH is structural remodeling of the small pulmonary vessels [2]. Proliferation of vascular smooth muscle, accumulation of extracellular matrix, and perivascular infiltrates of inflammatory cells are the main components of the remodeling process [2, 4].

Chronic inflammation is now considered an important feature of PH that contributes to the structural pulmonary-vessel remodeling [5]. Among immune mediators, chemokines, which control leukocyte trafficking and can activate resident vascular cells, are believed to play a major role [6, 7]. In PH, chemokines are secreted by inflammatory cells, as well as by resident vascular cells including pulmonary vascular endothelial and smooth-muscle cells [5]. Alterations in the expression and production of several chemokines such as CCL2/Monocyte chemoattractant protein 1 (MCP-1) [8], CX3CL1/Fractalkine [9], and CCL5/Regulated on Activation, Normal T-cell Expressed and Secreted (RANTES) [10] have been demonstrated in severe PH and shown to predominate within the pulmonary vascular lesions. Delineating the role and importance of chemokines involved in the pulmonary vascular remodeling process is therefore essential to the identification of specific therapeutic targets within the chemokine system. As several chemokines may activate a single receptor, the role for chemokines is best assessed through their receptor-mediated effects.

The G-protein-coupled receptor CCR5 acts as a co-receptor required for HIV cell entry and is therefore a therapeutic target in HIV infection [11, 12]. New CCR5 antagonists have been developed [13, 14]. Whether these antagonists may slow the progression of HIV-associated PH and perhaps of other forms of PH deserves evaluation. CCR5 is activated upon stimulation by the CCR5 ligands CCL3 (MIP-1α), CCL4 (MIP-1β), and CCL5 (RANTES) and is strongly expressed on the principal cell types implicated in PH progression, including endothelial cells (ECs), smooth-muscle cells (SMCs), T cells, and macrophages [6, 7, 15, 16]. Moreover, CCL5 overexpression has been demonstrated within the pulmonary vascular wall

of patients with idiopathic PH [10]. That the CCR5 pathway plays an important role in atherosclerotic lesion formation is now well established, and several studies have documented protection against vascular lesions via inhibition of CCR5-mediated effects [6, 17]. Of note, several studies suggest a role in the pathogenesis of vascular injury for several HIV proteins, most notably HIV1 gp120, which binds directly to CCR5 [18-20].

The potential role for inflammatory processes in human PH, together with the importance of CCR5 in HIV infection and potentially in HIV-related PH or PH due to other causes, prompted us to investigate the CCR5 pathways in the pulmonary vascular remodeling process. To this end, we used several approaches: we evaluated CCR5 expression and localization in lung tissue from patients with PH; $CCR5^{-/-}$ mice exposed to chronic hypoxia; and the effect of maraviroc-induced CCR5 inhibition on PH induced in mice by exposure to chronic hypoxia or SU5416/hypoxia. For these studies, we used CCR5 knock-in mice expressing human CCR5, as maraviroc does not bind to murine CCR5 [21-23] and we also conducted cell studies in bone marrow (BM)-chimeric mice generated from $CCR5^{-/-}$ and wild-type (WT) mice, to investigate whether the CCL5-CCR5 pathway led to PH through direct effects on pulmonary vascular cells or through cross-talk between macrophages and pulmonary-artery smooth muscle cells (PA-SMCs).

Methods

Patients

Human lung tissue was obtained from 6 patients with idiopathic pulmonary artery hypertension who underwent lung transplantation at the University Hospital of Leuven, Belgium. The study protocol was approved by the Institutional Ethics Committee of the University Hospital of Leuven under agreement #S51577, and written informed consent was obtained from each patient. Control lung tissue was obtained from 6 patients undergoing lung resection surgery for localized lung tumors at the Montsouris Mutualist Institute in Paris, France. The controls had an FEV1/FVC ratio greater than 70%; none of the patients or controls had chronic cardiovascular, hepatic, or renal disease or a history of cancer chemotherapy. This study was approved by the institutional review board of the Henri Mondor Teaching Hospital (Creteil, France). All controls signed an informed consent document before study inclusion. Pulmonary tissue was snap frozen then stored at −80°C until use. Lung tissue samples collected during surgery were used for in situ immunohistochemical studies and CCR5 protein level determinations. PA-SMCs were isolated from control lung tissues.

Macaque tissue analysis

Lung tissues were collected from Chinese rhesus macaques infected 1 year earlier with SIV Δ-B670. SIV-infected macaques reported previously to exhibit increased pulmonary artery pressure due to histopathological changes in the pulmonary vessels were used for CCR5 immunohistochemical analysis in comparison with controls [24].

Mouse models

CCR5-deficient, h-CCR5ki, WT C57Bl/6j mice are described in the online supplemental methods section. Bone-marrow (BM) chimera were generated (see online supplemental methods) and maintained under pathogen-free conditions at the functional investigations animal facility at the Pitié-Salpêtrière Teaching Hospital, Paris, France [25]. The experiments were performed under agreement #94-28245 at a level-2 animal platform at the INSERM-Unit 955, Créteil, France.

Exposure to chronic hypoxia

Male mice aged 3 months were exposed to chronic hypoxia (9% O_2) in a ventilated chamber (Biospherix, New York, NY) [26]. The hypoxic environment was a mixture of air and nitrogen. The chamber was opened daily for 1 hour if drug treatment was necessary and twice a week otherwise to replenish the food and water supplies and clean the cages. Mice subjected to SU5416/hypoxia received an intraperitoneal injection of SU5416 20 mg/Kg once a week during hypoxia exposure. Maraviroc obtained from Pfizer was administered daily by oral gavage (200 mg/Kg).

Hemodynamics and ventricular weight measurements

At the specified time points after hypoxia exposure, mice were anesthetized, and hemodynamic and ventricular weight measurements were performed as previously described [26].

Antibodies, recombinant proteins, reagents

Antibodies for immunohistochemistry, Western-Blot, and fluorescence-activated cell sorting (FACS); as well as recombinant proteins (CCL5 and, gp120) and SU5416 are described in the online supplemental methods section.

Mouse lung tissue analysis

Lung tissue sections for immunostaining and immunolabeling were prepared as described in the online supplemental methods section. Total RNA and protein were extracted from the right lung of each animal. Total RNA was used for real-time PCR and total protein for Western blot and ELISA. The immunostaining, Western-Blot, ELISA, and real-time PCR methods are described in the online supplemental methods section.

Flow cytometry

Lungs, BAL cells preparation and FACS analysis are performed as previously described [27,17]. The methods are detailed in the supplemental data section.

Cells studies

Cultured human and mouse PA-SMCs were isolated by enzymatic digestion using a mix of collagenase and elastase as previously described [28, 29]. Alveolar macrophages from BAL fluid were obtained and cultured as previously described [27]. Serum-free conditioned media from BAL macrophages were collected after incubation for 24 h. Human PA-SMC proliferation was assessed by BrdU incorporation using the Cell Proliferation Elisa BrdU kit

(Roche Diagnostics, Meylan, France) according to the manufacturer's instructions. Mouse PA-SMC cell proliferation was assessed by MTT assay as previously described[29]. Intracellular free calcium concentrations were measured in FURA-2 loaded cells using a 340/380 fluorescence ratio [28, 30] (see online supplemental methods).

Assessment of pulmonary vascular remodeling and wall thickness

Standard procedures were used to assess the morphologic characteristics of pulmonary muscular arteries in lung-tissue sections stained with hematoxylin-eosin (HE). Vascular remodeling and wall thickness were assessed as previously described [26].

Statistical analysis

Quantitative variables from animal studies are reported as median and individual values. These variables were compared using the nonparametric Kruskal-Wallis test followed by the Mann-Whitney post-hoc test with Bonferroni's correction for multiple comparisons. Data from cell studies are reported as mean±SEM and compared using the Mann-Whitney test with Bonferroni's correction. For qPCR data, the values were normalized and a Wilcoxon rank-sum test was performed. P values<0.05 were considered significant

Results

Expression of CCR5 was increased in lungs from patients with iPH, mice with hypoxia-induced PH, and SIV-infected macaques

In explanted lungs from patients with idiopathic PH, we found marked increases in CCR5 protein levels compared with healthy donor lungs (Figure 1A). Immunofluorescence staining for CCR5 protein in lung tissues from the patients predominated in PA-SMCs from the hypertrophied media of pulmonary vessels, ECs, and macrophages, as shown by double-immunofluorescence staining for CCR5 and α smooth muscle actin (α-SMA), von Willebrand factor (vWF), and CD68, respectively, of paraffin-embedded lung sections (Figure 1B, C and D). CCR5 immunostaining was more marked in areas characterized by greater severity of medial hypertrophy. Immunostaining for CCR5, which was markedly increased in remodeled pulmonary vessels from SIV-infected macaques compared to controls, also predominated in the hypertrophied medial layer (Supplemental Figure 1).

We then evaluated the expression of CCR5 and its ligands in lungs from wild-type (WT) mice developing hypoxic PH. Hypoxia exposure was followed by progressive increases in right ventricular systolic pressure (RVSP) and in the RV hypertrophy index (RV weight/left ventricle + septum weight [LV+S]), which became significant on day 3 compared with control normoxic mice then continued until day 18 (Figure 2A). Lung CCR5 mRNA levels were increased on day 3 and remained elevated until day 18 of hypoxia exposure (Figure 2B). CCL3, CCL4, and CCL5 mRNA levels were also elevated on day 3 (Figure 2B), and the corresponding protein levels increased from day 8 to day 18 (Figure 2C).

CCR5 gene deficiency abrogates the development of hypoxic PH in mice

Our finding of CCR5 overexpression in PH prompted us to test whether CCR5 gene deletion altered PH development in mice. After hypoxia exposure for 18 days, RVSP was

significantly lower and right ventricular hypertrophy less severe in CCR5$^{-/-}$ mutants than in WT mice (Figure 3A). Furthermore, distal pulmonary vessels exhibited less muscularization in CCR5$^{-/-}$ than in WT mice, with a smaller percentage of dividing Ki67-positive pulmonary vascular cells (Figure 3A). In both CCR5$^{-/-}$ and WT mice, the total number of lung macrophages determined by either flow cytometry (Figure 3B) or immunohistochemical analysis (data not shown) remained unchanged after 18 days of hypoxia exposure and did not differ between mouse strains. However, the number of macrophages surrounding pulmonary vessels (Figure 3C) or present in bronchoalveolar lavage (BAL) fluid (Figure 3D), which did not differ between CCR5$^{-/-}$ and WT mice under normoxic conditions, increased markedly from normoxia to hypoxia in WT mice but not in CCR5$^{-/-}$ mice. Consistent with decreased perivascular and alveolar macrophage recruitment, CCR5$^{-/-}$ mice had lower counts of lung inflammatory (CCR2^{hi}) monocytes, but not of constitutive (CX3CR1^{hi}) monocytes, compared to WT mice, during both normoxia and hypoxia (Supplemental Figure 2).

Maraviroc-induced CCR5 inhibition protects against PH development in human-CCR5ki mice

We hypothesized that pharmacological CCR5 inhibition with maraviroc altered PH development. Because maraviroc does not bind to murine CCR5 [21-23], we used CCR5 knock-in mice expressing human CCR5 (h-CCR5ki) for pharmacological studies and immunohistochemical analyses of CCR5-expressing cells. After 18 days of hypoxia, the h-CCR5ki mice had similar PH severity to that in WT mice and showed large increases in lung CCR5 protein levels (Figure 4A) and CCR5 staining in the PA-SMC layer of remodeled vessels (Figure 4B), whereas CCR5 staining in PA-ECs and macrophages was less affected by PH development (Figure 4C and D). Maraviroc 200 mg/Kg/day markedly attenuated, but did not fully abrogate, PH development as assessed by RVSP, RV/LV+S, and distal pulmonary artery muscularization in chronically hypoxic h-CCR5ki mice (Figure 5A); this treatment had no effect in WT mice. The protective effect of maraviroc in h-CCR5ki mice coincided with a decrease in the percentage of Ki67-positive cells (Figure 5A). Consistent with our findings in WT and CCR5$^{-/-}$ mice, we found that the total lung macrophage count remained unchanged after 18 days of hypoxia exposure, with no effect of maraviroc treatment (Figure 5B). In contrast, perivascular and BAL-fluid macrophage numbers were substantially decreased by maraviroc treatment in hypoxic h-CCR5ki mice and unchanged in hypoxic WT mice (Figure 5C and D). In contrast to our finding in CCR5$^{-/-}$ mice, lung-monocyte subset counts were unaltered by maraviroc in h-CCR5ki mice (data not shown). Similar effects of maraviroc on PH severity were obtained in another model of PH induced in mice by simultaneous hypoxia exposure and treatment with the VEGF receptor inhibitor SU5416 (Supplemental Figure 3). In addition to its preventive effect, maraviroc from day 15 to day 30 partially reversed PH in chronically hypoxic mice (Supplemental Figure 4).

Hypoxic PH development is altered in bone marrow-chimeric mice generated from CCR5$^{-/-}$ and WT mice

Given the potential effect on PH of alveolar macrophages recruited during hypoxia exposure, we assessed the effects of bone marrow (BM) transplantation on hypoxic PH in CCR5$^{-/-}$ and WT mice. WT and CCR5$^{-/-}$ mice received BM cells from WT or CCR5$^{-/-}$

donors. As shown in Figure 6A, strong protection against hypoxic PH was observed in $CCR5^{-/-}$ mice reconstituted with WT BM cells, compared to control WT mice reconstituted with WT BM cells, suggesting prominent CCR5-mediated effects on PA-SMCs. These protective effects were associated with a marked decrease in the number of macrophages surrounding lung microvessels (Figure 6B). Of note, $CCR5^{-/-}$ mice reconstituted with $CCR5^{-/-}$versus WT BM cells did not differ regarding PH parameters. However, WT mice reconstituted with $CCR5^{-/-}$ BM cells also benefited from some protection against PH when compared to WT mice reconstituted with WT BM cells and exhibited a significant decrease in perivascular macrophages (Figure 6B).

CCR5 activation leads to proliferation of cultured human PA-SMCs, which is inhibited by maraviroc

To establish that cultured human PA-SMCs express CCR5 protein, we performed a double immunostaining analysis for CCR5 and α-SMA (Figure 7 A). We found strong CCR5 immunostaining in all cultured PA-SMCs, which co-localized with the membrane-bound Transient Receptor Potential Channel 4 (TRPC4, Figure 7B). CCR5 expression increased in PA-SMCs exposed to hypoxia, and this effect was unaffected by maraviroc (Supplemental Figure 5). We next assessed the ability of CCL5 to induce proliferation of human PA-SMCs. CCL5 added to human PA-SMCs cultured in serum-free media produced a concentration-dependent increase in BrdU incorporation (Figure 7 C) that was not observed with similar concentrations of CCL3 or CCL4 (data not shown). Of note, mouse and human recombinant CCL5 produced similar levels of human PA-SMC stimulation (data not shown). Cell pretreatment with maraviroc (10 μM) completely abolished PA-SMC growth induced by CCL5 but did not affect growth induced by platelet-derived growth factor (PGDF, Figure 7 D). Because SMC proliferation requires intracellular calcium mobilization, we then analyzed the ability of CCL5 to increase the PA-SMC cytoplasmic calcium concentration $[Ca^{2+}]_i$, as a means of determining whether PA-SMC CCR5 was functionally coupled. CCL5 induced a transient $[Ca^{2+}]_i$ increase in cells cultured in Ca^{2+}-free medium (Figure 7 E and H). Cell pretreatment with maraviroc (10 μM) completely abolished $[Ca^{2+}]_i$ changes induced by CCL5, whereas the transient $[Ca^{2+}]_i$ increased by PDGF was not abrogated by maraviroc (Figure 7 E, G and H).

In addition, we found that treatment of human PA-SMCs with picomolar concentrations of the HIV1 protein gp120 also stimulated growth and increased intracellular calcium, both responses being inhibited by maraviroc (Figure 7 D, F and H). The heat-inactivated gp120 was without effects (Supplemental Figure 6).

Alveolar macrophages contribute to CCR5-mediated PA-SMC proliferation

We then examined the effects of CCL5 on mouse PA-SMCs. CCL5 stimulated the growth of PASMCs derived from WT and h-CCR5ki mice but, in contrast to PDGF, failed to alter PASMCs from $CCR5^{-/-}$ mice (Supplemental Figure 7). In h-CCR5ki and WT mice, CCL5 produced a concentration-dependent increase in cell proliferation that was not observed with similar concentrations of CCL3 or CCL4 (data not shown). Of note, mouse and human recombinant CCL5 stimulated h-CCR5ki PA-SMC cells similarly (data not shown). Cell pretreatment with maraviroc (10 μM) completely abolished the growth-promoting effect of

CCL5 on PA-SMCs derived from h-CCR5ki mice but not from WT mice (Supplemental Figure 7). Similarly, maraviroc abolished the migration of h-CCR5ki cells but not of WT cells stimulated by CCL5 (Supplemental Figure 8).

To investigate whether lung macrophages contributed to PA-SMC growth, we assessed the effects of conditioned medium (CM) from cultured alveolar macrophages on PA-SMC growth. Compared to CCL5, supernatants of alveolar macrophages from WT mice induced greater stimulation of h-CCR5ki PA-SMC proliferation (Figure 8A). Maraviroc treatment abolished PA-SMC proliferation induced by CCL5 and attenuated that induced by macrophage-conditioned media (Figure 8A). The CCL5 level in macrophage-conditioned media from hypoxic mice was increased compared to those from normoxic mice (Supplemental Figure 9). However, compared to normoxic macrophage CM, hypoxic macrophage CM did not induce greater cell proliferation (data not shown).

We then evaluated whether CCR5-mediated macrophage stimulation promoted the growth of cultured PA-SMCs. To this end, we used macrophages from h-CCR5ki mice and PA-SMCs from WT mice. As shown in Figure 8B, CCL5 potentiated the PA-SMC growth-promoting effects of alveolar macrophages, and this effect was slightly reduced by maraviroc. As expected, maraviroc did not affect CCL5-induced proliferation of PA-SMCs from WT mice.

Discussion

The role for chemokines and chemokine receptors in PH progression is receiving considerable attention. The recent addition of CCR5 receptor antagonists to the treatment armamentarium for HIV infection prompted us to evaluate the CCR5 receptor. To assess the role for CCR5 in experimental PH, we used both gene disruption and pharmacological CCR5 inactivation in mice. CCR5 receptor antagonists such as maraviroc do not bind to murine CCR5 and we therefore used h-CCR5ki mice for pharmacological studies and immunohistochemical analyses of CCR5-expressing cells. Using a combination of studies on human lung tissues and derived cultured cells, macaque lung tissues, transgenic mouse models, and mouse cells, we demonstrated that CCR5 activation in PA-SMCs and lung macrophages played a major role in PH progression.

Our findings provide strong support for CCR5 inhibition as a novel therapeutic approach in PH. Marked upregulation of the CCR5 receptor was found in our PH patients. As previously emphasized, inflammation is a common feature in human PH that is not targeted by any of the current treatments. An important point when considering chemokines as targets for PH treatment is that some ligand-receptor pairs are involved in activating not only inflammatory cells, but also constitutive vascular cells directly involved in the remodeling process [6]. We found that CCR5 in lungs from patients with PH was strongly expressed, not only by lung macrophages, but also by PA-SMCs and PA-ECs, most notably at sites of intense vascular remodeling. Moreover, strong CCR5 immunostaining was detected in the media of pulmonary vessels from SIV-infected macaques exhibiting marked pathological changes [24]. Although previous studies documented CCR5 expression by systemic vessels [6], a potential

direct role for CCR5 in the pathogenesis and progression of PH had not been considered previously.

Here, we used the well-known animal model of hypoxic PH, in which inflammation is considered a potential contributor [31]. In most species, hypoxia exposure immediately induces overexpression of inflammatory mediators such as CCL2, IL-6, and IL-1β, which usually precedes the development of hypoxic PH [31]. In some species such as rats and neonatal calves, increased counts of lung macrophages and neutrophils have also been reported [31]. In mice, hypoxia was recently shown to be associated with early macrophage accumulation around the pulmonary vessels and in BAL fluid, and this accumulation was linked to the pulmonary remodeling process [27]. The role for inflammation in hypoxic PH, however, remains unclear, since specific cytokine-receptor pathways appear to have opposite effects [8, 32, 33].

We found that lung CCR5 and CCR5 ligands increased early after hypoxia exposure then remained elevated during PH development. CCR5 immunolocalization in h-CCR5ki mice was similar to that in human lungs, with prominent staining of the pulmonary vessel walls and macrophages. A major finding from our study is that either genetic deletion or pharmacological inhibition of CCR5 protected against PH development, with an effect of maraviroc treatment in two experimental models, hypoxia- and SU5416/hypoxia-induced PH. Both $CCR5^{-/-}$ mice and h-CCR5ki mice treated with maraviroc exhibit attenuations in PH severity with decreases in both distal pulmonary artery muscularization and dividing Ki67-positive PA-SMCs. Interestingly, these effects were not associated with changes in total counts of lung macrophages or lung monocyte subsets. However, the macrophage counts around vessels and in BAL fluid, which increased during hypoxia exposure, were lower in $CCR5^{-/-}$ mice compared to WT mice and decreased with maraviroc treatment in h-CCR5ki mice, suggesting a contribution of CCR5 to macrophage recruitment during hypoxia exposure. Thus, pharmacological inhibition or genetic deletion of CCR5 produced similar effects, markedly diminishing pulmonary vascular remodeling and PA-SMC proliferation and also decreasing perivascular and alveolar macrophage counts.

CCR5 exerted a strong functional effect on PA-SMCs when stimulated by CCR5 ligands in low physiological concentrations. Our finding that CCL5 was more potent than CCL3 or CCL4 for activating PA-SMCs is consistent with the differences in CCR5 ligand efficacy across cell types [7]. PA-SMCs from h-CCR5ki and WT mice responded similarly to CCL5, indicating that CCR5-mediated signals did not depend on the human or murine origin of CCR5. Our results also show that maraviroc binds only to human CCR5, since CCL5-induced activation of human and h-CCR5ki PA-SMCs, but not of WT PA-SMCs, was completely suppressed by maraviroc. Thus, the close similarities between results from human and h-CCR5ki tissues and cells in terms of CCR5 localization, expression, and functional activities are consistent with a major role for the CCL5/CCR5 pathway in mediating pulmonary vascular remodeling through direct PA-SMC activation. In keeping with such a role, protection against PH was similar in $CCR5^{-/-}$ mice reconstituted with WT BM and in $CCR5^{-/-}$ mice reconstituted with $CCR5^{-/-}$ BM cells. These results are consistent with a prominent effect of CCR5-mediated signals on resident lung cells and more specifically on PA-SMCs, given the decrease in dividing Ki67-positive cells within the

pulmonary vessel media. In addition, we found that the HIV1 envelope protein gp120, which is known to bind to CCR5,[19] also stimulated PA-SMC growth and calcium signaling, and that both effects were inhibited by maraviroc. Of note, we used gp120 protein in concentrations recently found in several organs from HIV-infected patients [34]. These results therefore suggest that, in HIV-infected patients, maraviroc may inhibit both CCL5-CCR5 and gp120-CCR5 signaling in PASMCs.

As mentioned before, several studies recently documented a link between activated lung macrophages and the development of PH, particularly of hypoxic PH in mice [27, 31]. In our study, perivascular and alveolar macrophage counts were diminished in maraviroc-treated mice and in $CCR5^{-/-}$ mice, although lung levels of CCR5 ligands either remained unchanged or increased, suggesting decreased lung macrophage recruitment related to CCR5 inactivation. Consistent with this possibility, WT mice reconstituted with $CCR5^{-/-}$ BM cells showed substantial protection from PH, together with decreased perivascular macrophage counts, supporting a role for BM-derived inflammatory cells possibly mediated by the CCL5/CCR5 pathway. Our finding that lung macrophages were the main cell type strongly expressing CCR5 in addition to vascular cells supports a contribution of these cells to PH through the CCL5/CCR5 pathway.

CM from alveolar macrophages stimulated PA-SMC growth, and this effect was only partially inhibited by maraviroc, suggesting that macrophages released growth-promoting mediators other than CCL5 [27]. Also, the growth of WT PA-SMCs exposed to conditioned media of CCL5-stimulated macrophages from h-CCR5ki mice was increased compared to vehicle-treated macrophages, indicating that the CCL5/CCR5 pathway contributed to activate the monocyte/macrophage lineage involved in pulmonary vascular remodeling during PH progression. However, this effect was only slightly altered by maraviroc treatment, a finding consistent with the fact that CCL5 activation of alveolar macrophages can be mediated by receptors other than CCR5 [7]. Taken together, these results indicate that the CCL5-CCR5 pathway plays a major role in the pulmonary vascular remodeling process through both direct PA-SMC activation and lung macrophage recruitment and activation.

These findings are highly relevant to the clinical management of patients with PH. That chronic maraviroc treatment markedly attenuated the development of hypoxic PH in h-CCR5ki mice but had no effect in WT mice indicates that maraviroc protected against PH by specifically binding to human CCR5 and was devoid of CCR5-independent effects. Moreover, we chose the maraviroc dose for our in vivo studies in h-CCR5ki mice based on the plasma levels achieved in humans. Thus, our results are consistent with a pharmacological action of maraviroc in humans, in whom the drug blocks the CCR5 receptor in micromolar plasma concentrations [13]. These findings carry major implications for the treatment of HIV-related PH, whose clinical presentation and underlying pathology are similar to those of idiopathic or associated PH and whose prevalence in HIV-infected patients is 1000-fold higher than the prevalence of idiopathic PH in the general population [3]. Moreover, several studies of vascular-injury pathogenesis in HIV-infected patients have implicated HIV proteins, most notably gp120, which binds to CCR5 [19, 20]. Our results showing a growth-stimulating effect of gp120 on human PA-SMCs and its inhibition by maraviroc may be of major clinical relevance. CCR5 inhibitors may therefore be of

considerable clinical benefit in HIV-infected patients who develop PH. They should be considered for addition to other antiretroviral therapies such as HIV protease inhibitors, which we have previously shown to interfere with the pathophysiology of PH [35].

The identification of specific therapeutic targets in the chemokine system is crucial to the development of treatments that counteract the progression of PH due to various causes. Our results also support the potential usefulness of CCR5 inhibition in patients with other forms of PH. We characterized specific roles for the CCL5/CCR5 pathway in mediating pulmonary vascular remodeling, using a CCR5-receptor antagonist designed to inhibit HIV cell entry. Thus, using available drugs to block the CCR5 signaling pathway might benefit patients with PH complicating HIV infection or with other forms of PH.

Supplementary Material

Refer to Web version on PubMed Central for supplementary material.

Acknowledgments

The authors thank Richard Souktani for the Level 2 animal platform, Mehdi Latiri for mouse PA-SMC culture and animal experimentation, Bijan Ghaleh for using the hypoxia cell chamber, and Pierre Validire from the Montsouris Mutualist Institute for providing us human pulmonary artery specimens.

Funding Sources: This study was supported by grants from the INSERM, Fondation pour la Recherche Médicale, Ministère de la Recherche, Association Française contre les Myopathies (AFM 16442), Chancellerie des Universités de Paris, Fondation Cœur-poumon, DHU ATVB, and European Grant ENDOSTEM (FP7 241440). Dr. Combadière receives research support from AFM: Chemomyo project. Dr. Norris and Dr. Gladwin receive research support from NIH grant P01HL103455 for studies of PAH in SIV infection.

References

1. Simonneau G, Robbins IM, Beghetti M, Channick RN, Delcroix M, Denton CP, Elliott CG, Gaine SP, Gladwin MT, Jing ZC, Krowka MJ, Langleben D, Nakanishi N, Souza R. Updated clinical classification of pulmonary hypertension. J Am Coll Cardiol. 2009; 54:S43–54. [PubMed: 19555858]
2. Tuder RM, Marecki JC, Richter A, Fijalkowska I, Flores S. Pathology of pulmonary hypertension. Clin Chest Med. 2007; 28:23–42. vii. [PubMed: 17338926]
3. Sitbon O, Lascoux-Combe C, Delfraissy JF, Yeni PG, Raffi F, De Zuttere D, Gressin V, Clerson P, Sereni D, Simonneau G. Prevalence of HIV-related pulmonary arterial hypertension in the current antiretroviral therapy era. Am J Respir Crit Care Med. 2008; 177:108–113. [PubMed: 17932378]
4. Morrell NW, Adnot S, Archer SL, Dupuis J, Jones PL, MacLean MR, McMurtry IF, Stenmark KR, Thistlethwaite PA, Weissmann N, Yuan JX, Weir EK. Cellular and molecular basis of pulmonary arterial hypertension. J Am Coll Cardiol. 2009; 54:S20–31. [PubMed: 19555855]
5. Hassoun PM, Mouthon L, Barbera JA, Eddahibi S, Flores SC, Grimminger F, Jones PL, Maitland ML, Michelakis ED, Morrell NW, Newman JH, Rabinovitch M, Schermuly R, Stenmark KR, Voelkel NF, Yuan JX, Humbert M. Inflammation, growth factors, and pulmonary vascular remodeling. J Am Coll Cardiol. 2009; 54:S10–19. [PubMed: 19555853]
6. Schober A. Chemokines in vascular dysfunction and remodeling. Arterioscler Thromb Vasc Biol. 2008; 28:1950–1959. [PubMed: 18818421]
7. Charo IF, Ransohoff RM. The many roles of chemokines and chemokine receptors in inflammation. N Engl J Med. 2006; 354:610–621. [PubMed: 16467548]
8. Sanchez O, Marcos E, Perros F, Fadel E, Tu L, Humbert M, Dartevelle P, Simonneau G, Adnot S, Eddahibi S. Role of endothelium-derived CC chemokine ligand 2 in idiopathic pulmonary arterial hypertension. Am J Respir Crit Care Med. 2007; 176:1041–1047. [PubMed: 17823354]

9. Balabanian K, Foussat A, Dorfmuller P, Durand-Gasselin I, Capel F, Bouchet-Delbos L, Portier A, Marfaing-Koka A, Krzysiek R, Rimaniol AC, Simonneau G, Emilie D, Humbert M. CX(3)C Chemokine Fractalkine in Pulmonary Arterial Hypertension. Am J Respir Crit Care Med. 2002; 165:1419–1425. [PubMed: 12016106]
10. Dorfmuller P, Zarka V, Durand-Gasselin I, Monti G, Balabanian K, Garcia G, Capron F, Coulomb-Lhermine A, Marfaing-Koka A, Simonneau G, Emilie D, Humbert M. Chemokine RANTES in severe pulmonary arterial hypertension. Am J Respir Crit Care Med. 2002; 165:534–539. [PubMed: 11850348]
11. Dragic T, Litwin V, Allaway GP, Martin SR, Huang Y, Nagashima KA, Cayanan C, Maddon PJ, Koup RA, Moore JP, Paxton WA. HIV-1 entry into CD4+ cells is mediated by the chemokine receptor CC-CKR-5. Nature. 1996; 381:667–673. [PubMed: 8649512]
12. Deng H, Liu R, Ellmeier W, Choe S, Unutmaz D, Burkhart M, Di Marzio P, Marmon S, Sutton RE, Hill CM, Davis CB, Peiper SC, Schall TJ, Littman DR, Landau NR. Identification of a major co-receptor for primary isolates of HIV-1. Nature. 1996; 381:661–666. [PubMed: 8649511]
13. Ray N. Maraviroc in the treatment of HIV infection. Drug Des Devel Ther. 2009; 2:151–161.
14. Henrich TJ, Kuritzkes DR. HIV-1 entry inhibitors: recent development and clinical use. Curr Opin Virol. 2013; 3:51–57. [PubMed: 23290628]
15. Schecter AD, Calderon TM, Berman AB, McManus CM, Fallon JT, Rossikhina M, Zhao W, Christ G, Berman JW, Taubman MB. Human vascular smooth muscle cells possess functional CCR5. J Biol Chem. 2000; 275:5466–5471. [PubMed: 10681524]
16. Ishida Y, Kimura A, Kuninaka Y, Inui M, Matsushima K, Mukaida N, Kondo T. Pivotal role of the CCL5/CCR5 interaction for recruitment of endothelial progenitor cells in mouse wound healing. J Clin Invest. 2012; 122:711–721. [PubMed: 22214846]
17. Combadiere C, Potteaux S, Rodero M, Simon T, Pezard A, Esposito B, Merval R, Proudfoot A, Tedgui A, Mallat Z. Combined inhibition of CCL2, CX3CR1, and CCR5 abrogates Ly6C(hi) and Ly6C(lo) monocytosis and almost abolishes atherosclerosis in hypercholesterolemic mice. Circulation. 2008; 117:1649–1657. [PubMed: 18347211]
18. Kanmogne GD, Schall K, Leibhart J, Knipe B, Gendelman HE, Persidsky Y. HIV-1 gp120 compromises blood-brain barrier integrity and enhances monocyte migration across blood-brain barrier: implication for viral neuropathogenesis. J Cereb Blood Flow Metab. 2007; 27:123–134. [PubMed: 16685256]
19. Hill CM, Deng H, Unutmaz D, Kewalramani VN, Bastiani L, Gorny MK, Zolla-Pazner S, Littman DR. Envelope glycoproteins from human immunodeficiency virus types 1 and 2 and simian immunodeficiency virus can use human CCR5 as a coreceptor for viral entry and make direct CD4-dependent interactions with this chemokine receptor. J Virol. 1997; 71:6296–6304. [PubMed: 9261346]
20. Lund AK, Lucero J, Herbert L, Liu Y, Naik JS. Human immunodeficiency virus transgenic rats exhibit pulmonary hypertension. Am J Physiol Lung Cell Mol Physiol. 2011; 301:L315–326. [PubMed: 21685241]
21. Saita Y, Kondo M, Shimizu Y. Species selectivity of small-molecular antagonists for the CCR5 chemokine receptor. Int Immunopharmacol. 2007; 7:1528–1534. [PubMed: 17920529]
22. Mansfield R, Able S, Griffin P, Irvine B, James I, Macartney M, Miller K, Mills J, Napier C, Navratilova I, Perros M, Rickett G, Root H, van der Ryst E, Westby M, Dorr P. CCR5 pharmacology methodologies and associated applications. Methods Enzymol. 2009; 460:17–55. [PubMed: 19446719]
23. Mansfield, RW.; Sale, HE.; Mosley, MJ.; Rickett, G.; Dorr, P.; Perros, M. UK-472,857 binding characteristics to human and animal recombinant CCR5 receptors. XV International AIDS Conference: WePeA5640; 2009.
24. George MP, Champion HC, Simon M, Guyach S, Tarantelli R, Kling HM, Brower A, Janssen C, Murphy J, Carney JP, Morris A, Gladwin MT, Norris KA. Physiologic changes in a nonhuman primate model of HIV-associated pulmonary arterial hypertension. Am J Respir Cell Mol Biol. 2013; 48:374–381. [PubMed: 23239493]
25. Potteaux S, Combadiere C, Esposito B, Lecureuil C, Ait-Oufella H, Merval R, Ardouin P, Tedgui A, Mallat Z. Role of bone marrow-derived CC-chemokine receptor 5 in the development of

atherosclerosis of low-density lipoprotein receptor knockout mice. Arterioscler Thromb Vasc Biol. 2006; 26:1858–1863. [PubMed: 16763157]

26. Mouraret N, Marcos E, Abid S, Gary-Bobo G, Saker M, Houssaini A, Dubois-Rande JL, Boyer L, Boczkowski J, Derumeaux G, Amsellem V, Adnot S. Activation of lung p53 by Nutlin-3a prevents and reverses experimental pulmonary hypertension. Circulation. 2013; 127:1664–1676. [PubMed: 23513067]
27. Vergadi E, Chang MS, Lee C, Liang OD, Liu X, Fernandez-Gonzalez A, Mitsialis SA, Kourembanas S. Early macrophage recruitment and alternative activation are critical for the later development of hypoxia-induced pulmonary hypertension. Circulation. 2011; 123:1986–1995. [PubMed: 21518986]
28. Bobe R, Hadri L, Lopez JJ, Sassi Y, Atassi F, Karakikes I, Liang L, Limon I, Lompre AM, Hatem SN, Hajjar RJ, Lipskaia L. SERCA2a controls the mode of agonist-induced intracellular Ca2+ signal, transcription factor NFAT and proliferation in human vascular smooth muscle cells. J Mol Cell Cardiol. 2011; 50:621–633. [PubMed: 21195084]
29. Abid S, Houssaini A, Mouraret N, Marcos E, Amsellem V, Wan F, Dubois-Rande JL, Derumeaux G, Boczkowski J, Motterlini R, Adnot S. P21-dependent protective effects of a carbon monoxide-releasing molecule-3 in pulmonary hypertension. Arterioscler Thromb Vasc Biol. 2014; 34:304–312. [PubMed: 24334871]
30. Lipskaia L, Hadri L, Le Prince P, Esposito B, Atassi F, Liang L, Glorian M, Limon I, Lompre AM, Lehoux S, Hajjar RJ. SERCA2a gene transfer prevents intimal proliferation in an organ culture of human internal mammary artery. Gene Ther. 2013; 20:396–406. [PubMed: 22763406]
31. Stenmark KR, Fagan KA, Frid MG. Hypoxia-induced pulmonary vascular remodeling: cellular and molecular mechanisms. Circ Res. 2006; 99:675–691. [PubMed: 17008597]
32. Perros F, Dorfmuller P, Souza R, Durand-Gasselin I, Godot V, Capel F, Adnot S, Eddahibi S, Mazmanian M, Fadel E, Herve P, Simonneau G, Emilie D, Humbert M. Fractalkine-induced smooth muscle cell proliferation in pulmonary hypertension. Eur Respir J. 2007; 29:937–943. [PubMed: 17182651]
33. Yu YR, Mao L, Piantadosi CA, Gunn MD. CCR2 deficiency, dysregulation of Notch signaling, and spontaneous pulmonary arterial hypertension. Am J Respir Cell Mol Biol. 2013; 48:647–654. [PubMed: 23492191]
34. Santosuosso M, Righi E, Lindstrom V, Leblanc PR, Poznansky MC. HIV-1 envelope protein gp120 is present at high concentrations in secondary lymphoid organs of individuals with chronic HIV-1 infection. J Infect Dis. 2009; 200:1050–1053. [PubMed: 19698075]
35. Gary-Bobo G, Houssaini A, Amsellem V, Rideau D, Pacaud P, Perrin A, Bregeon J, Marcos E, Dubois-Rande JL, Sitbon O, Savale L, Adnot S. Effects of HIV protease inhibitors on progression of monocrotaline- and hypoxia-induced pulmonary hypertension in rats. Circulation. 2010; 122:1937–1947. [PubMed: 20974998]

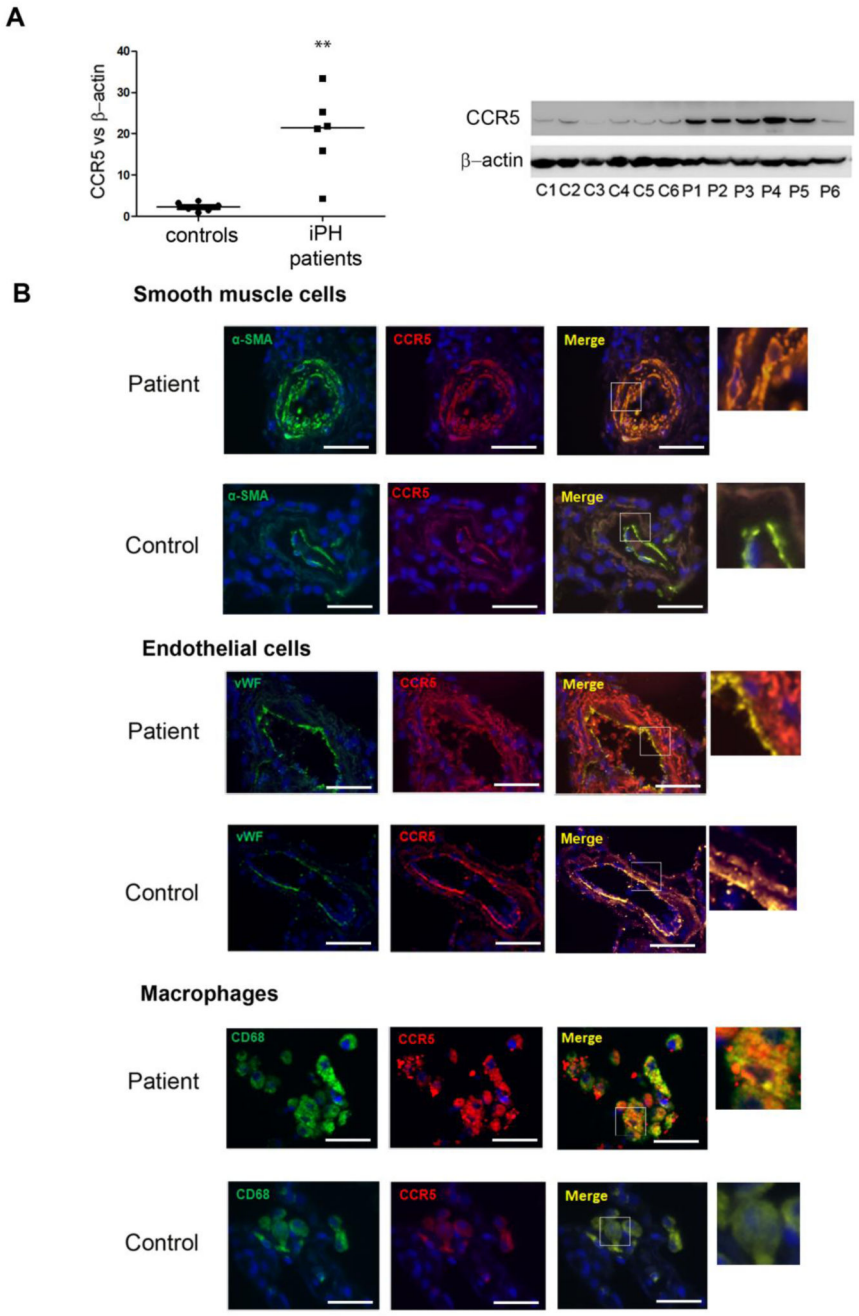

Figure 1.

Increased expression of CCR5 in human PH. (A)- CCR5 protein level measured by Western blot in total lung protein extracts from patients P1 to P6 with idiopathic PH (iPH) and controls C1 to C6. Individual values and median (black bar) from 6 patients and 6 ageand sex-matched controls. ***P*<0.01. (B)- Representative micrographs of lung tissue from patients and controls. CCR5 (Red), α-SMA for SMC staining, vWF for endothelial cell staining, CD68 for macrophage staining (Green), or Dapi for nucleus staining (Blue). No

positive immunoreactivity was detected in sections incubated with the appropriate control IgG followed by secondary anti-rabbit and anti-mouse antibodies. Bar=40 μm.

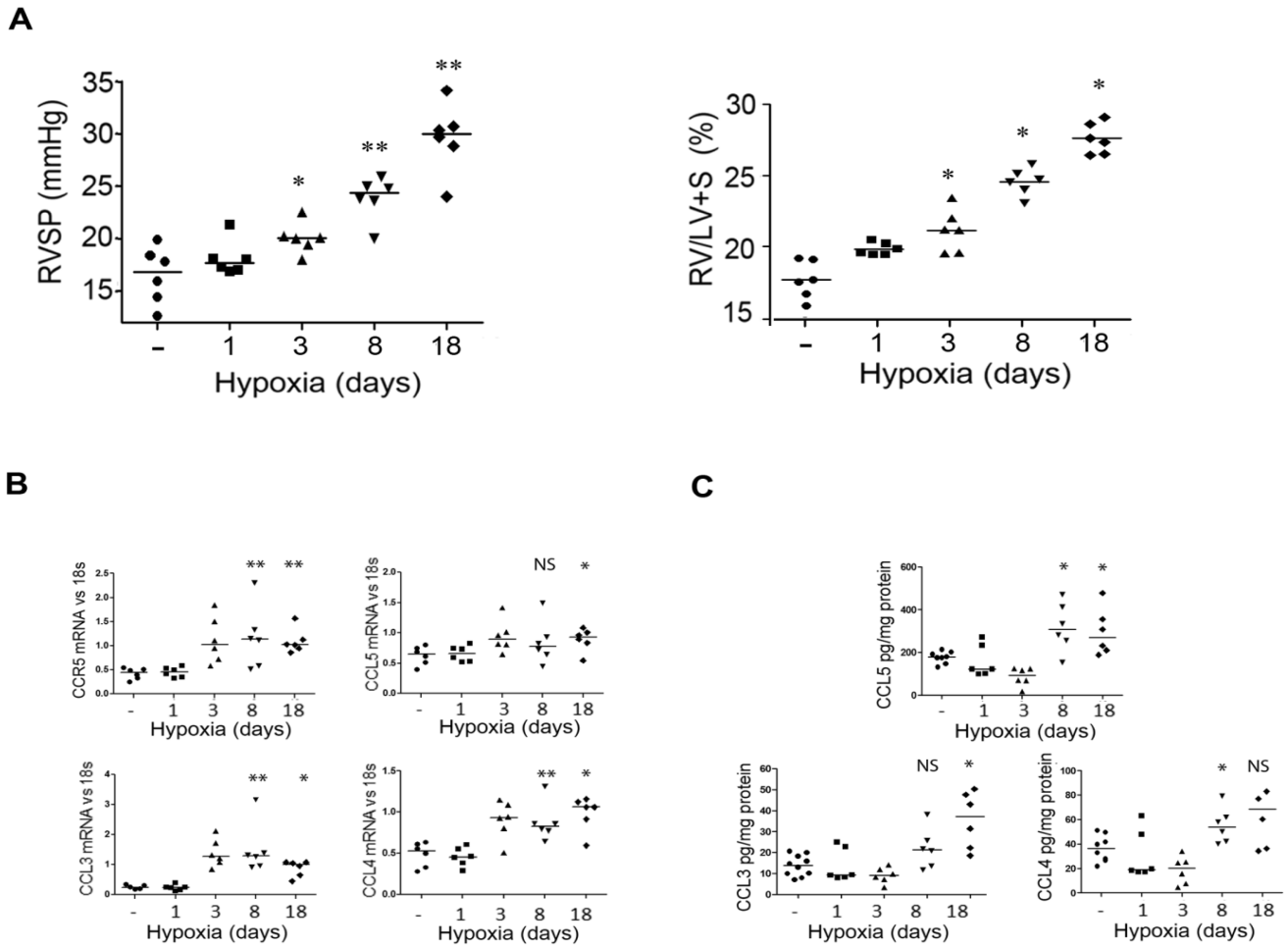

Figure 2.

Increased expression of CCR5 and its ligands in murine hypoxia-induced PH (A)- Effect of hypoxia on pulmonary hypertension development. Graphs of right ventricular systolic pressure (RVSP) and right ventricular hypertrophy index (RV/[left ventricle plus septum (LV+S)] weight) in wild-type mice exposed to hypoxia for various durations. Both individual and median values are shown. **P*<0.016, ***P*<0.0033 vs. normoxia. (B)- Lung mRNA levels for CCR5 and its ligands CCL5, CCL3 and CCL4 measured using quantitative RT-PCR after hypoxia exposure for various durations. Both individual and median values are shown. **P*<0.025, ***P*<0.005 vs. normoxia. (C)- Lung CCL5, CCL3 and CCL4 protein levels measured by ELISA. Both individual and median values are shown. **P*<0.025, ***P*<0.005 vs. normoxia.

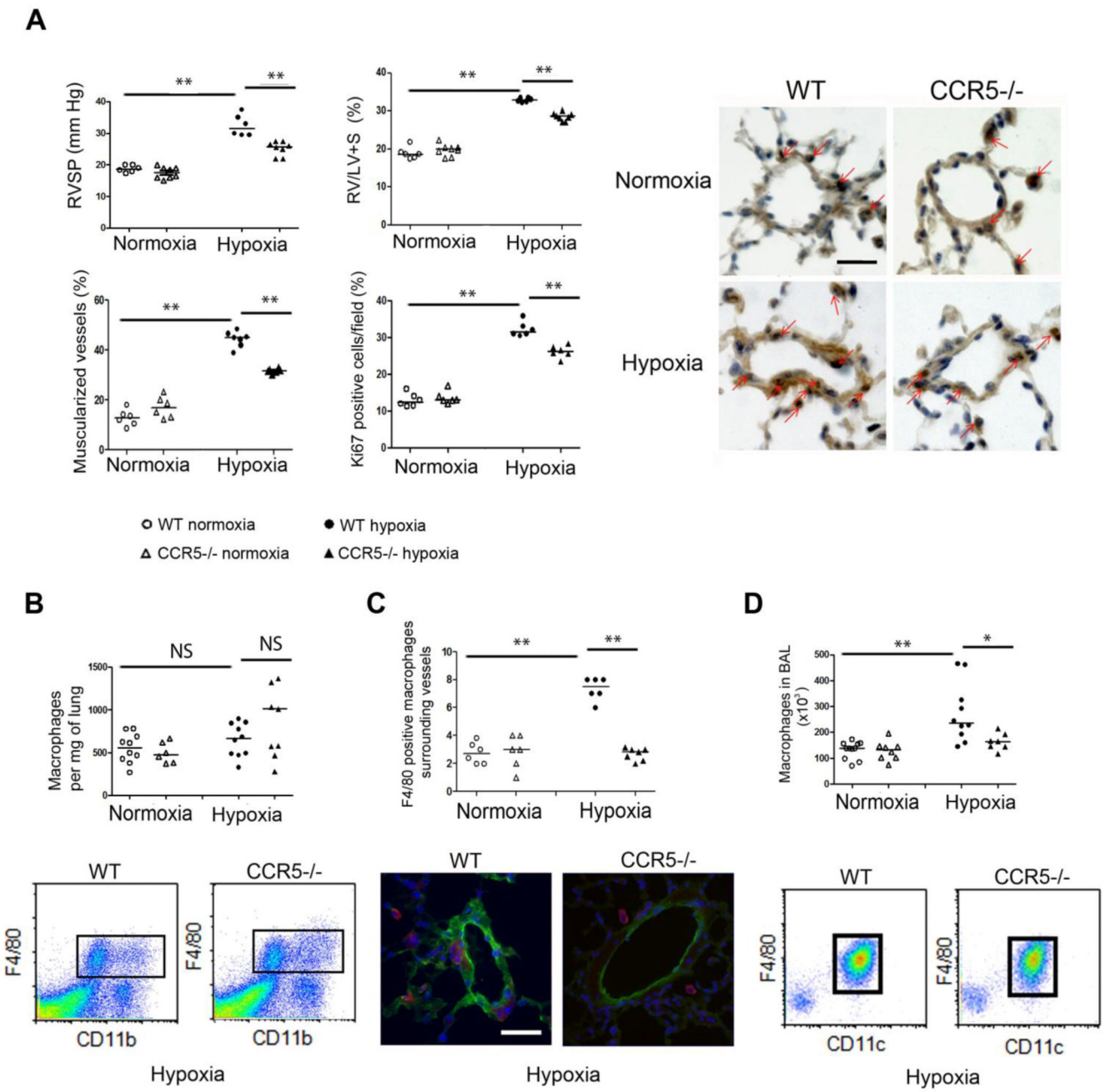

Figure 3.

CCR5 gene deficiency abrogates the development of hypoxic PH in mice. (A)- Graphs of right ventricular systolic pressure (RVSP) and right ventricular hypertrophy index (RV/[left ventricle plus septum (LV+S)] weight), pulmonary vessel muscularization, and dividing Ki67-positive cells in wild-type (WT) mice and CCR5$^{-/-}$ mice under normoxia and hypoxia. Representative micrographs of pulmonary vessels stained for Ki67 are shown in the right panel. Red arrows show Ki67-positive nuclei. No immunoreactivity was detected in sections incubated with rabbit IgG control and secondary anti-rabbit antibody. Bar=50 μm. (B)- Total macrophage counts in the lung. Graph shows the number of CD11b F4/80-positive

macrophages isolated from 1 mg of lung tissue and micrographs showing representative FACS profiles of cells from mouse lungs. (C)- Macrophage counts surrounding small pulmonary vessels. Graph shows the number of perivascular F4/80-positive macrophages detected using α-SMA staining. Micrographs show representative staining of macrophages surrounding lung vessels in WT and CCR5$^{-/-}$ mice under hypoxia; F4/80 (Red), α-SMA (Green), Dapi (Blue). No positive immunoreactivity was detected in sections incubated with control IgG followed by secondary anti-rabbit or anti-rat antibody. (D)- Macrophage counts in bronchoalveolar lavage (BAL) fluid. The graph shows the number of CD11c- and F4/80-positive macrophages. Micrographs show representative FACS profiles of BAL fluid cells from WT and CCR5 $^{-/-}$ mice under hypoxia. For all graph, both individual and median values are represented. * $P<0.025$ ** $P<0.005$.

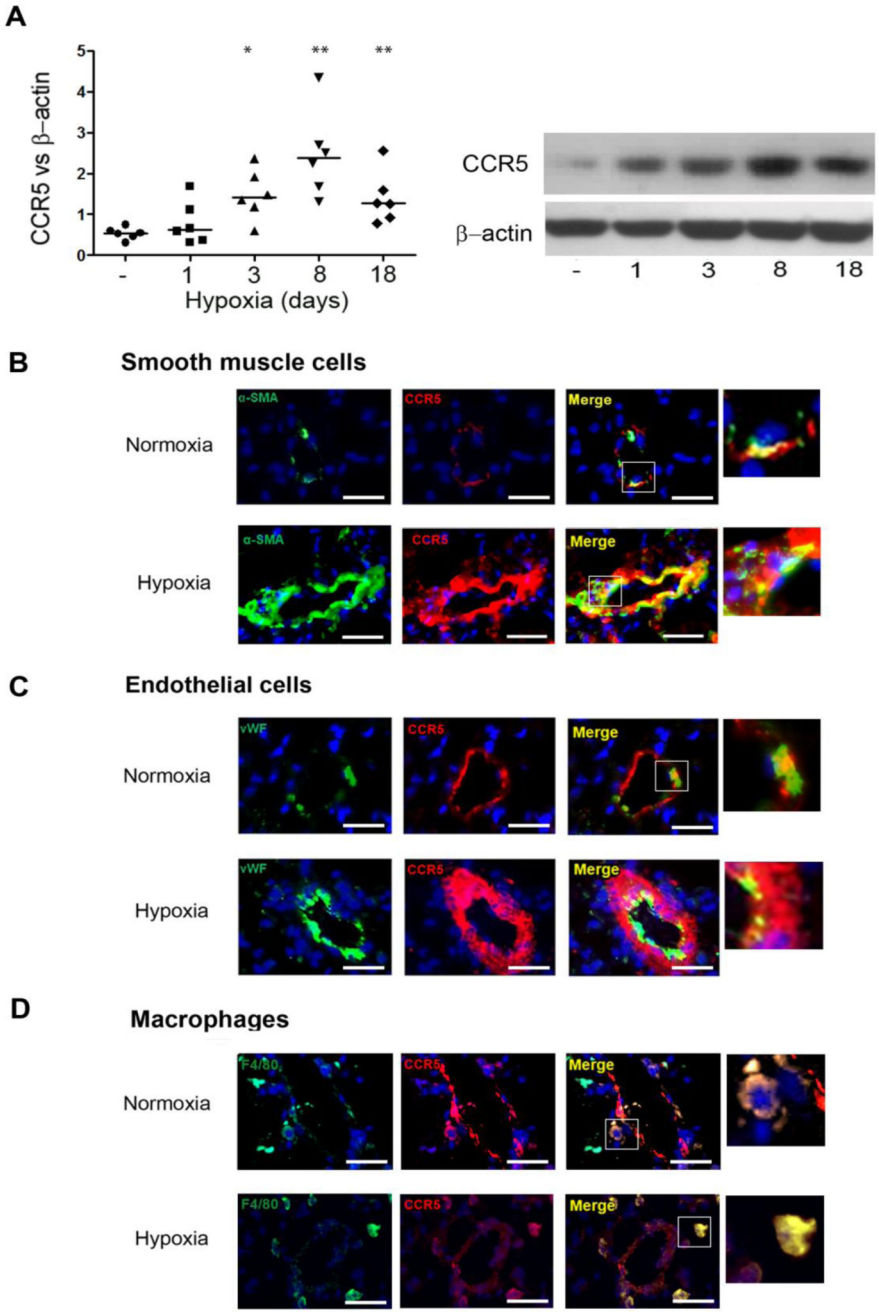

Figure 4.

Maraviroc-induced CCR5 inhibition protects against PH development in human-CCR5ki mice but not in wild-type (WT) mice. (A)- CCR5 expression during hypoxia exposure: CCR5 protein level measured by Western blot in lung tissue from h-CCR5ki mice under normoxia and after hypoxia exposure for various durations. Both individual and median values are represented. **P*<0.016, ***P*<0.0033 vs. normoxia. (B)- CCR5 (Red) co-localizes with SMCs. Lung sections from h-CCR5ki mice under normoxia and after 18 days of hypoxia were stained for CCR5 (Red) and α-SMA (Green). Nuclei were stained with Dapi

(Blue). (C)- CCR5 (Red) co-localized with ECs stained with vWF (Green). (D)- CCR5 (Red) co-localized with macrophages stained with Mac-3 (Green). No positive immunoreactivity was detected in sections incubated with the appropriate IgG control followed by secondary anti-rabbit and anti-mouse antibodies. Bar=25 μm

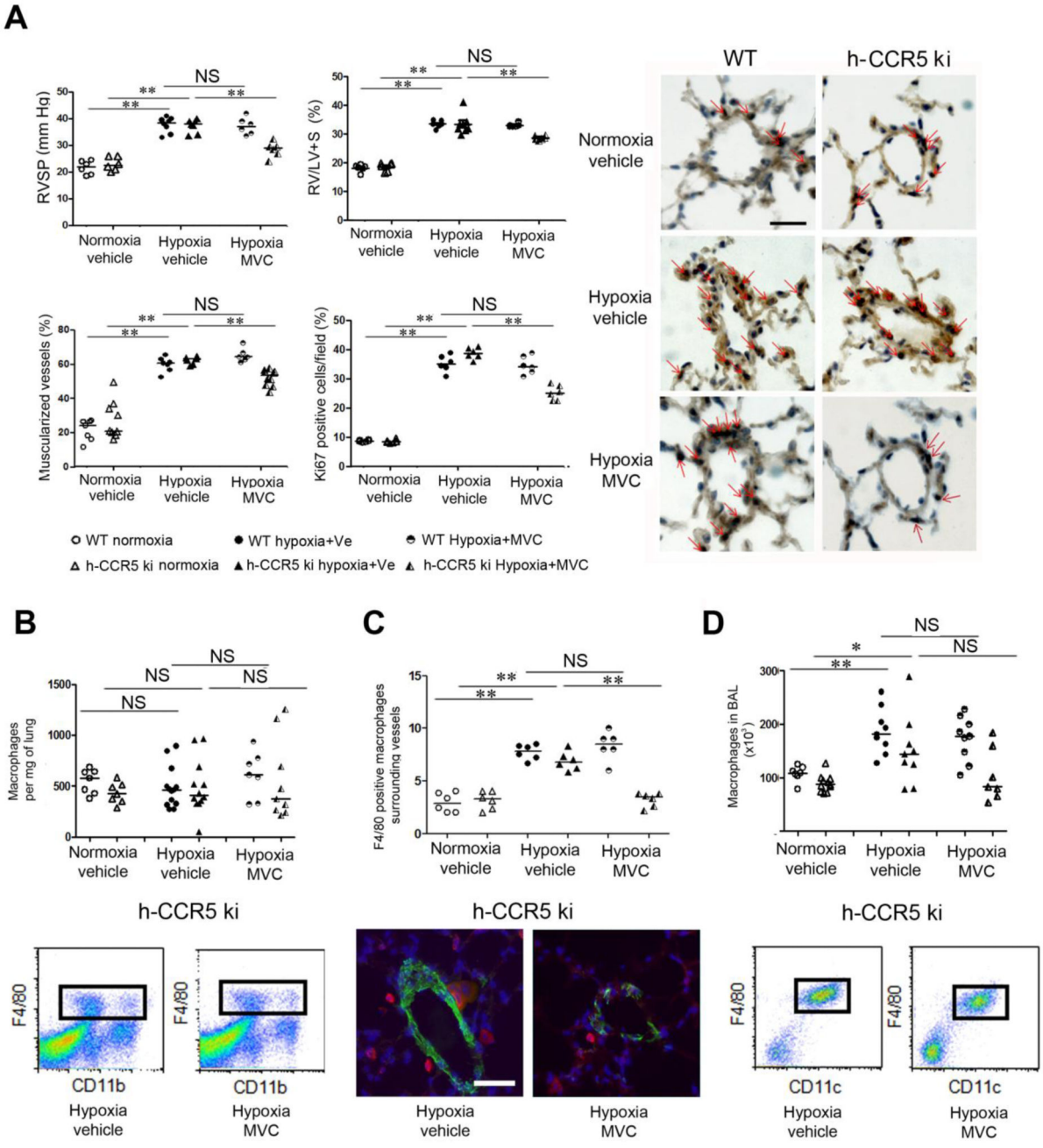

Figure 5.

Maraviroc-induced CCR5 inhibition protects against PH in CCR5ki mice but not in wild-type (WT) mice. (A)- Graphs of right ventricular systolic pressure (RVSP), right ventricular hypertrophy index (RV/(LV+S)] weight), pulmonary vessel muscularization, and percentages of dividing Ki67-positive cells in WT and h-CCR5ki mice treated daily with maraviroc (MVC) or vehicle (Ve) during hypoxia exposure. Representative micrographs of pulmonary vessels stained for Ki67 are shown in the right panel. Red arrows show Ki67-positive nuclei. No immunoreactivity was detected in sections incubated with rabbit IgG

control and secondary anti-rabbit antibody. Bar=50 μm. (B)- Total lung CD11b F4/80-positive macrophages and FACS profiles of cells from mouse lungs. (C)- Macrophage counts surrounding small pulmonary vessels (<100 μm) and micrographs showing representative staining of macrophages surrounding lung vessels in h-CCR5ki mice treated with MVC or vehicle: F4/80 (Red), α-SMA (Green), Dapi (Blue). (D)- Number of CD11c- and F4/80-positive macrophages in bronchoalveolar lavage (BAL) fluid and representative FACS profiles of BAL fluid cells from h-CCR5ki mice treated with MVC or vehicle. For all graph, both individual and median values are represented. * $P<0.025$, ** $P<0.005$. Values recorded during hypoxia did not differ between vehicle-treated WT and h-CCR5ki mice.

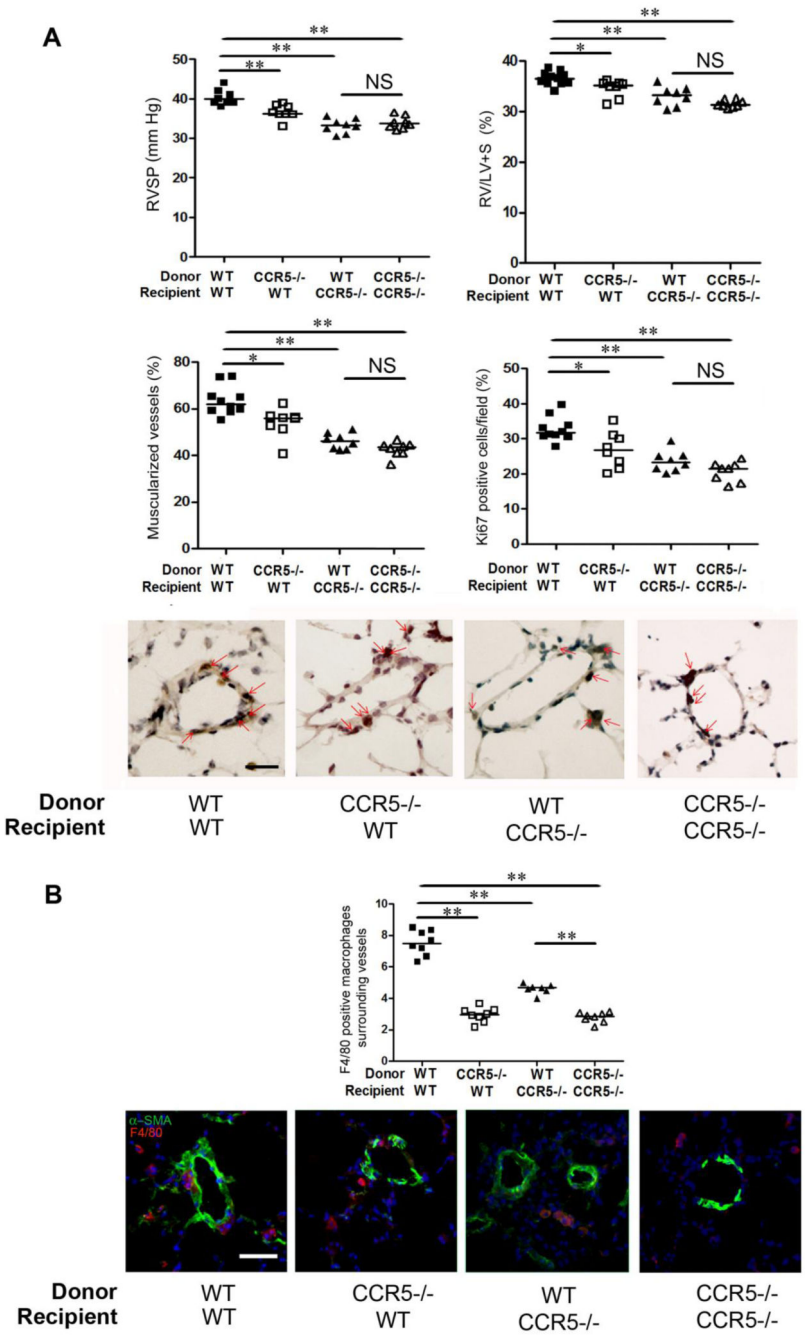

Figure 6.

Hypoxic PH development is altered in bone marrow-chimeric mice generated from CCR5$^{-/-}$ and wild-type (WT) mice. (A)- Graphs of right ventricular systolic pressure (RVSP) and right ventricular hypertrophy index (RV/[left ventricle plus septum (LV+S)] weight), pulmonary vessel muscularization, and percentages of dividing Ki67-positive cells in WT mice and CCR5$^{-/-}$ mice under normoxia or hypoxia. Representative micrographs of pulmonary vessels stained for Ki67. Bar=50 μm. No immunoreactivity was detected in sections incubated with rabbit IgG control and secondary anti-rabbit antibody. (B)- Graphs

of F4/80-positive macrophage counts around lung microvessels detected using α-SMA staining. Micrographs showing stained lung vessels surrounded with macrophages in WT and $CCR5^{-/-}$ mice under hypoxia; F4/80 (Red), α-SMA (Green), Dapi (Blue). No positive immunoreactivity was detected in sections incubated with the appropriate IgG control followed by secondary anti-rabbit and anti-rat antibodies. Bar=50 μm. For all graph, both individual and median values are represented. *P<0.016, **P<0.0033.

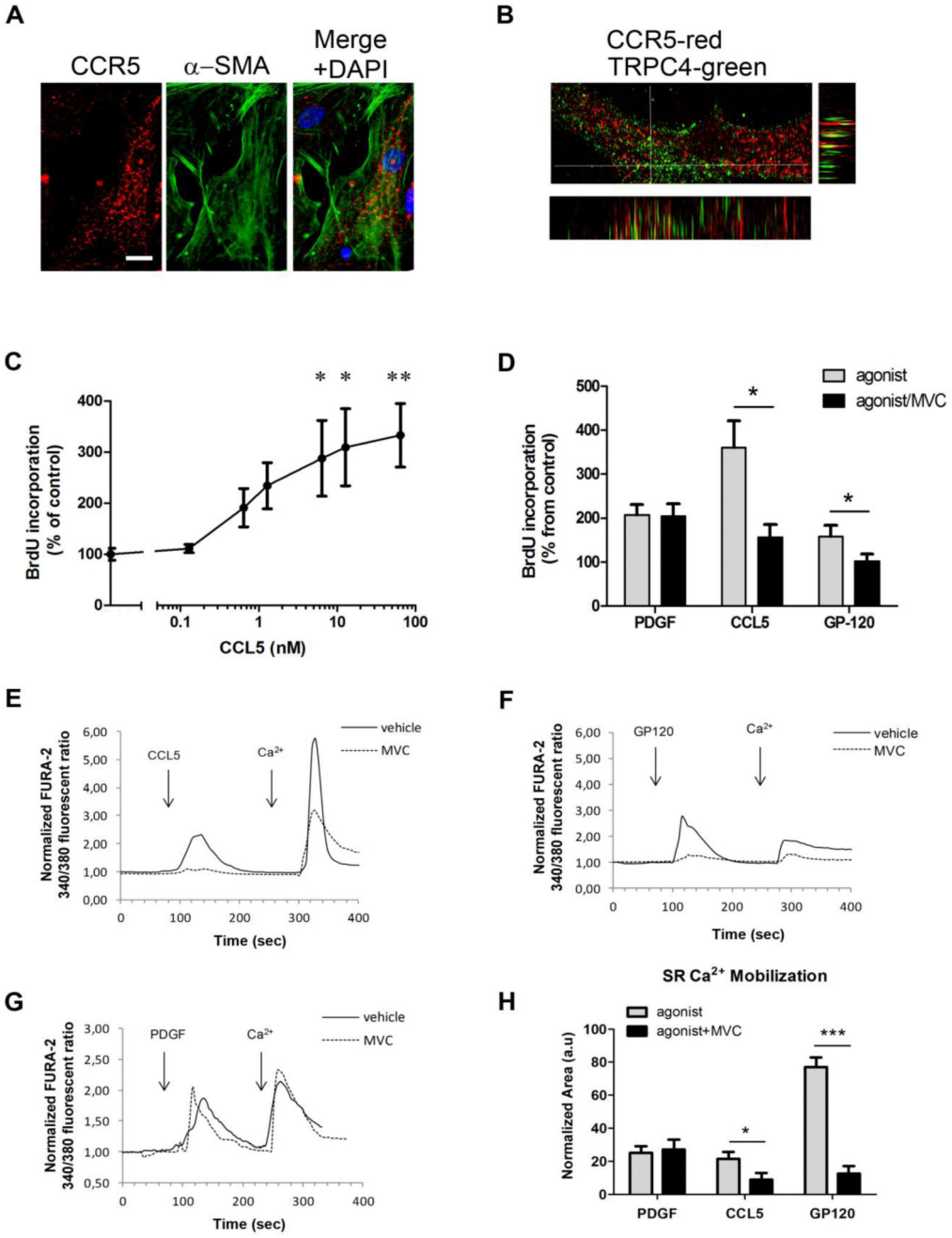

Figure 7.

Effect of CCR5 activation on intracellular calcium imaging and proliferation of PA-SMCs. (A)-Double immunolabeling of CCR5 (Red) and α-SMA (Green) in human PASMCs. Bar=10 μm. (B)- Double immunolabeling of CCR5 (Red) and TRPC4 (Green) in human PA-SMCs. Images at the bottom and left of the figure represent Z-stack orthogonal views of the cell at the positions of the horizontal and vertical bars, respectively. Co-localization of CCR5 and TRPC4 is indicated in yellow. (C)- Dose-response curve of the effect of CCL5 on human PA-SMC proliferation measured by BrdU incorporation. Data are mean±SEM of

10-15 values from at least three different experiments *P<0.0016, **P<0.0033 vs. vehicle. (D)- Effect of PDGF (50 ng/mL), CCL5 (10 nM) and gp120 (100 pM) on human PA-SMC proliferation in the presence of maraviroc (MVC: 10 μM) or vehicle. Data are mean±SEM of 10-15 values *P<0.05. (E.F,G) - Effects of CCL5 (10 nM), PDGF (50 ng/mL), and gp120 (100 pM) on intracellular calcium imaging in FURA-2 loaded cells in the presence of MVC (10 μM; dotted line) or vehicle (solid line). Each curve represents the mean of 10-20 cells from the same experiment. The capacity of the agonist to trigger Ca2+ mobilization from intracellular stores was assessed in the absence of extracellular calcium (EGTA 100 μM), and Ca2+ influx through plasma membrane channels was assessed after addition of extracellular Ca2+ (2 mM). (H)- Bar graph comparing the intracellular calcium peak induced by PDGF, CCL5, and gp120 with or without MVC. Data are mean±SEM of 25-100 cells from at least three different experiments *P<0.05; ***P<0.001.

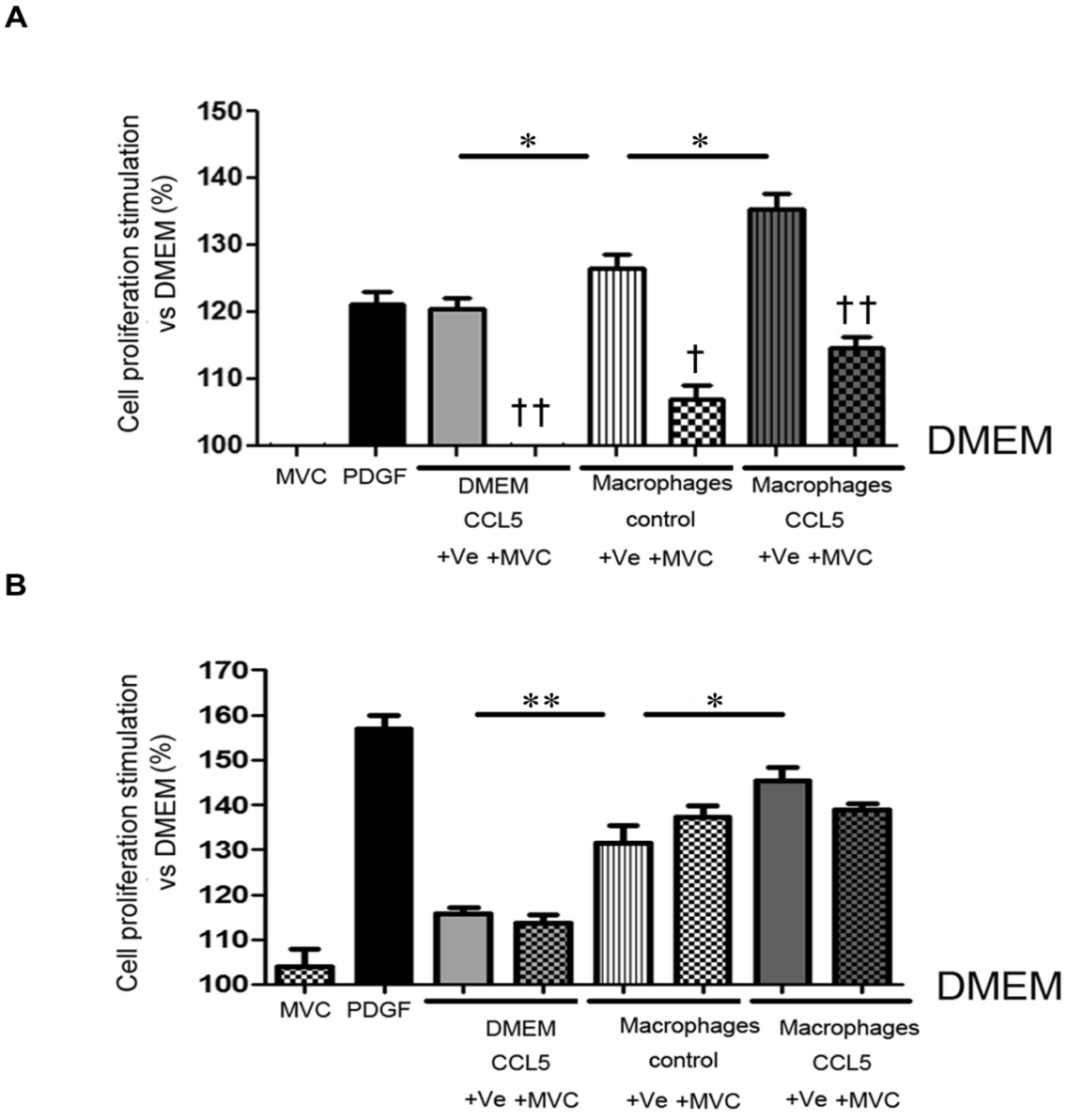

Figure 8.

Alveolar macrophages contribute to CCR5-mediated proliferation of pulmonary-artery smooth muscle cells (PA-SMCs). (A)- Effect of cultured WT alveolar-macrophage-conditioned media on h-CCR5ki PA-SMC proliferation. Values are expressed as percent of control values in DMEM starvation medium. Data are mean±SEM of 10-15 values from at least three different experiments. **P*<0.025; †*P*<0.01 ††*P*<0.001 for MVC vs. vehicle (Ve) under the same condition. (B)- Effect of cultured h-CCR5ki alveolar-macrophage-conditioned media on MVC-insensitive WT PA-SMC cell proliferation. Starved cultured macrophages were treated with CCL5 and Ve or MVC before collection of the conditioned media. Values are expressed as percent of control values in DMEM starvation medium. Data

are mean±SEM of 10-15 values from at least three different experiments.*P<0.025, **P<0.005.